Combining lidar and Thermal Infrared imagery to search for geothermal features in Oregon

Ian Madin, John English, Paul Ferro, Clark Niewendorp
Oregon Department of Geology and Mineral Industries

Summer Lake, Oregon Geothermal Imagery Project
Funded by ARRA via USDOE and AZ Geological Survey
The goal of this project was to test whether high resolution TIR and lidar imagery can find low amplitude thermal anomalies associated with blind geothermal systems

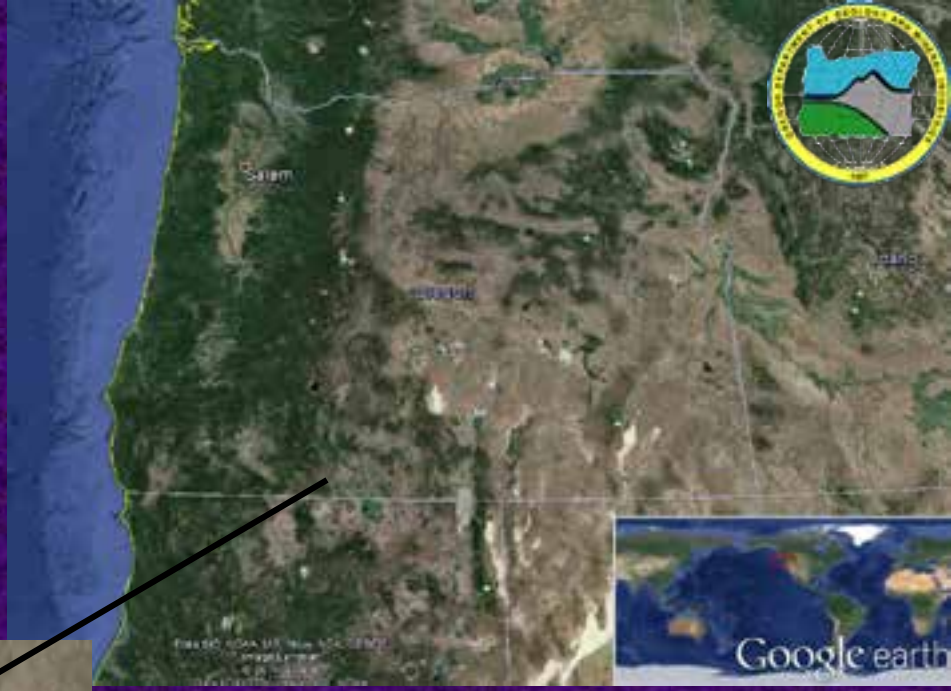

48 square miles
Acquired March 4 2012, 00:34-06:07 hours.
Ambient T during acquisition -8 to -5 C°
5.4 ppsm lidar, .25 m DEM 2cm RMSE vertical accuracy
0.5 m pixel, 0.5 C° thermal resolution TIR (8-9.2 um) imagery, mosaicked and orthorectified with lidar DEM
0.5 m RMSE horizontal accuracy
Collected by Watershed Sciences Inc.

ESRI UC 2014 Ian Madin

Calibrated Radiant Temperature (T_r) Map

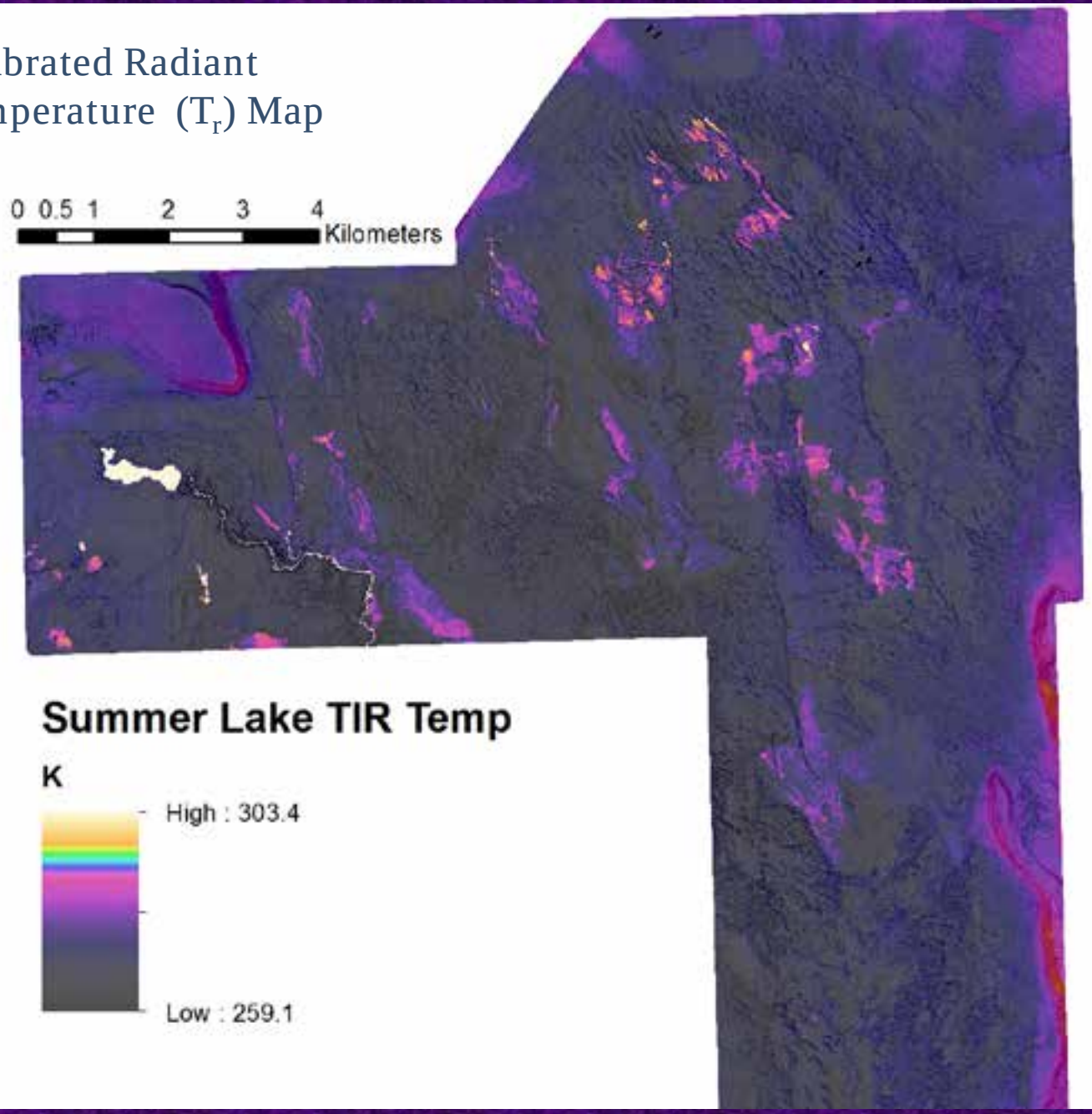

Locating warm and cold springs

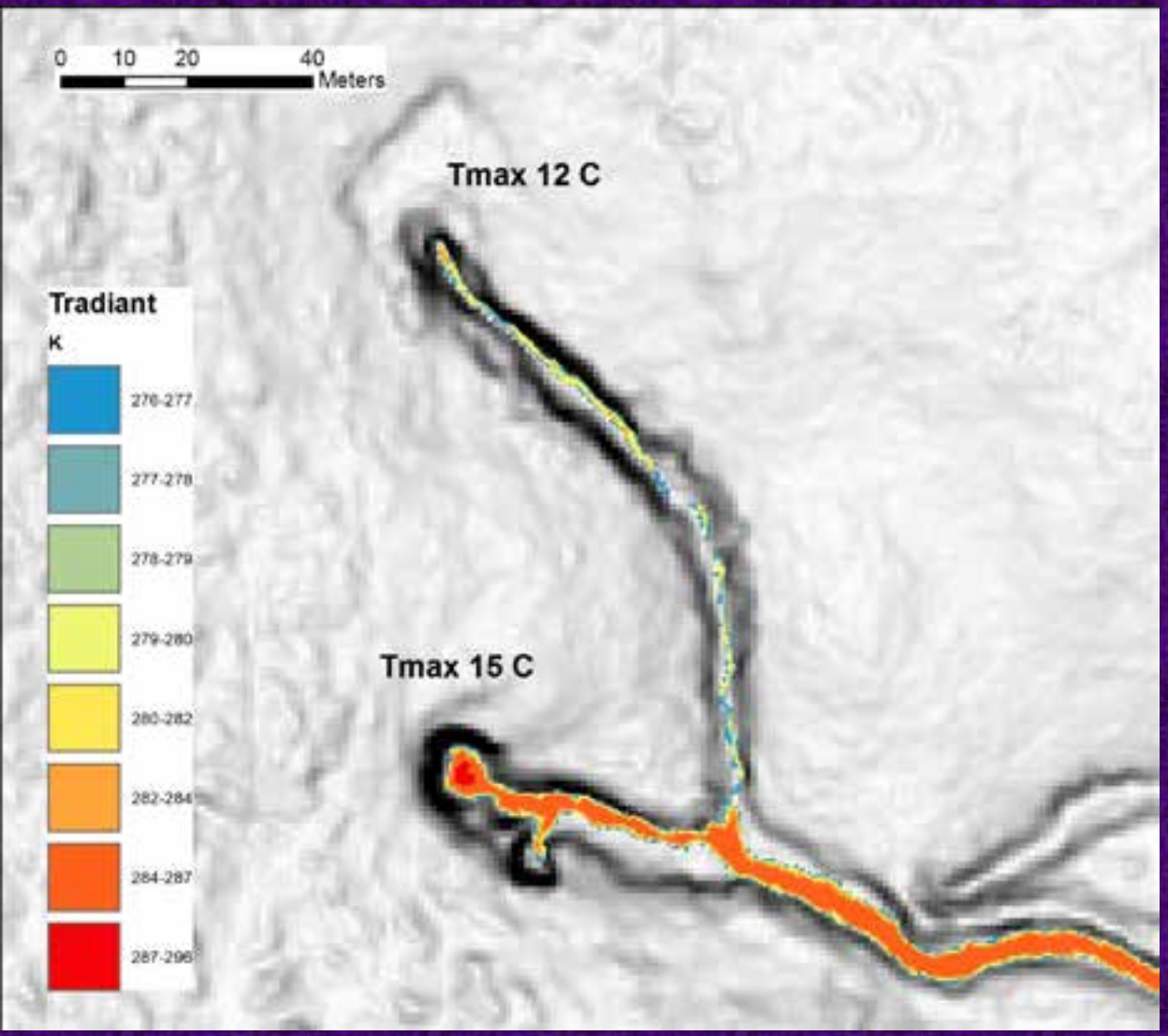

We used the close correspondence of the lidar topography and TIR and the high ε of water to locate springs and measure their temperature. We extracted all T_r values greater than 276 K, and examined the results in the context of the topography. Not only were springs easy to locate, it was easy to measure their temperature. This approach was very sensitive, identifying springs on the basis of as few as 4 pixels.

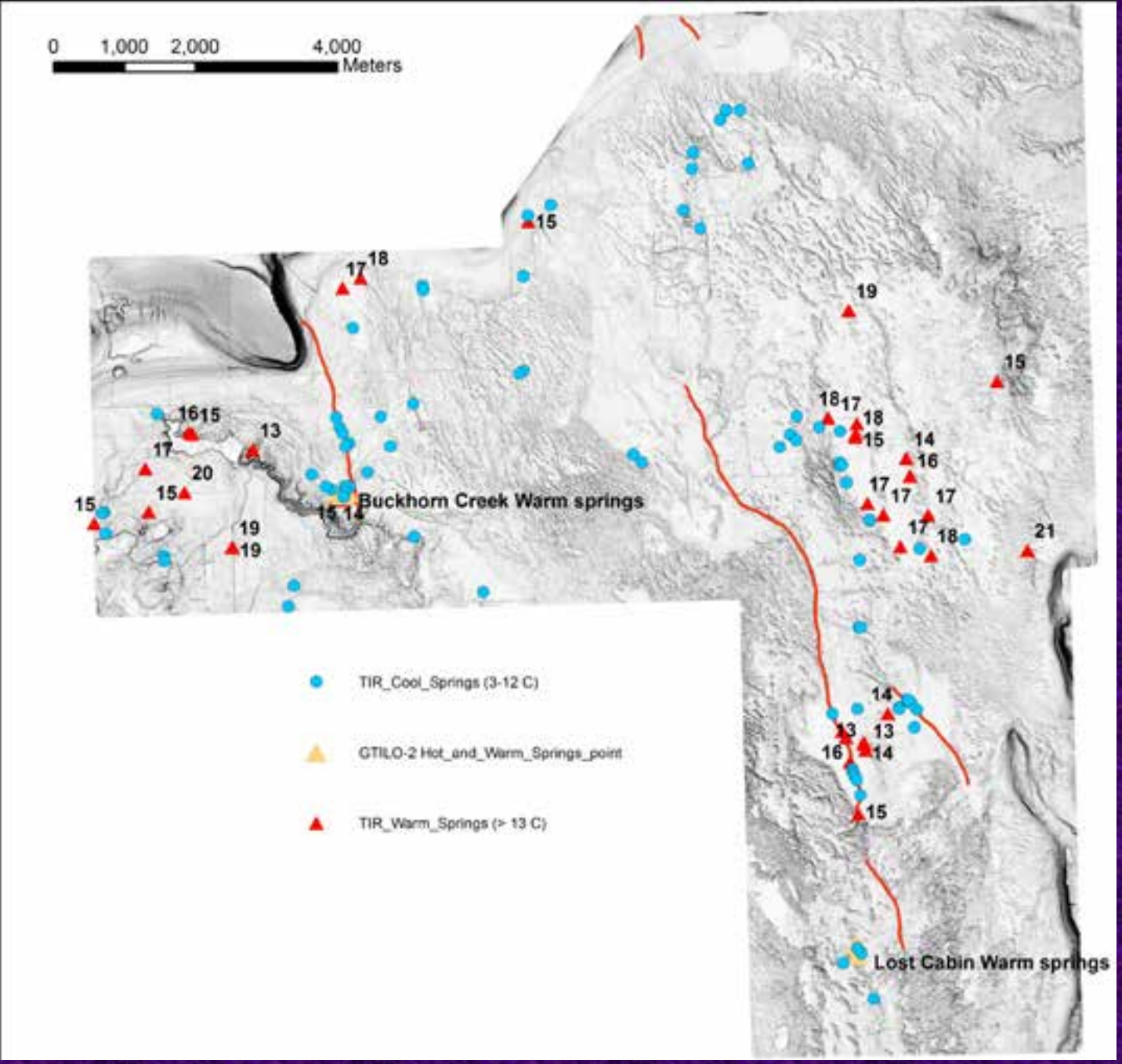

Not only were numerous warm springs found that were not in the geothermal database, several springs that were in the database were no longer flowing.

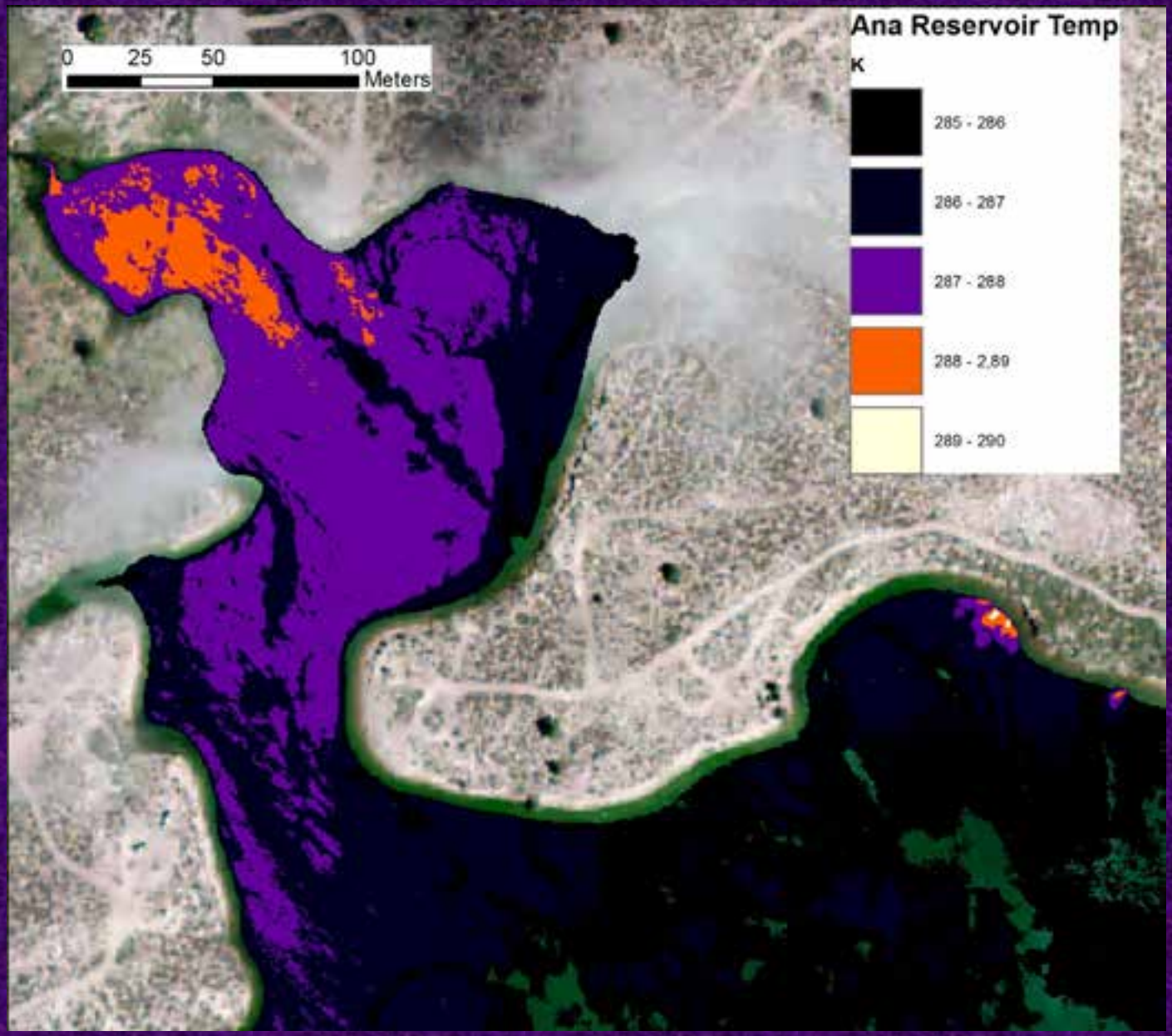

We were even able to identify warm springs within Ana Reservoir

The most prominent anomalies in the radiant temperature (T_r) map are associated with water bodies, bedrock cliffs and highlands, and vegetation
T_r is a function of the actual temperature of the surface ($T_{kinetic}$, or T_k) and its emissivity (ε) at the thermal wavelengths:

$$T_{radiant} = \varepsilon^{1/4} T_{kinetic}$$

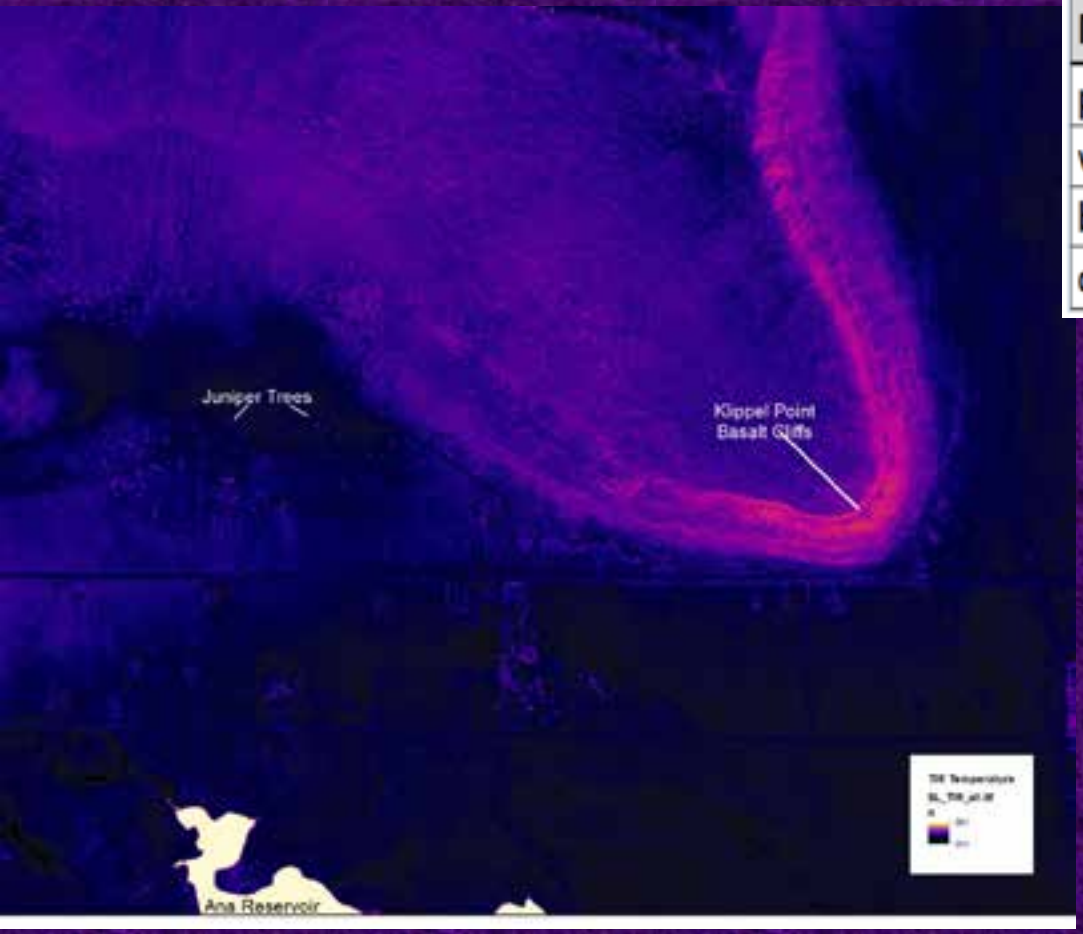

Material	$T_{kinetic}$	ε	$T_{radiant}$
pine	273	0.98	271.6
water	273	0.95	269.5
basalt	273	0.72	251.5
desert soil	273	0.9	265.9

ε varies dramatically between different materials, so even at the same T_k, water and juniper trees should appear hotter than soil or rock. Water really stands out because it is both warmer than the ambient temperatures, and because it has a high ε.
The bedrock highlands however should look colder at the same T_k.

Because the cliffs more directly face the low winter sun they might have absorbed more heat during the day than flat ground. To test this we used the insolation tools to calculate total insolation for the day preceding the collection. We used spatial analyst to calculate a correlation coefficient for the T_r raster and the insolation raster, and the resulting 0.07 value rules out insolation as a cause. These may be real thermal anomalies.

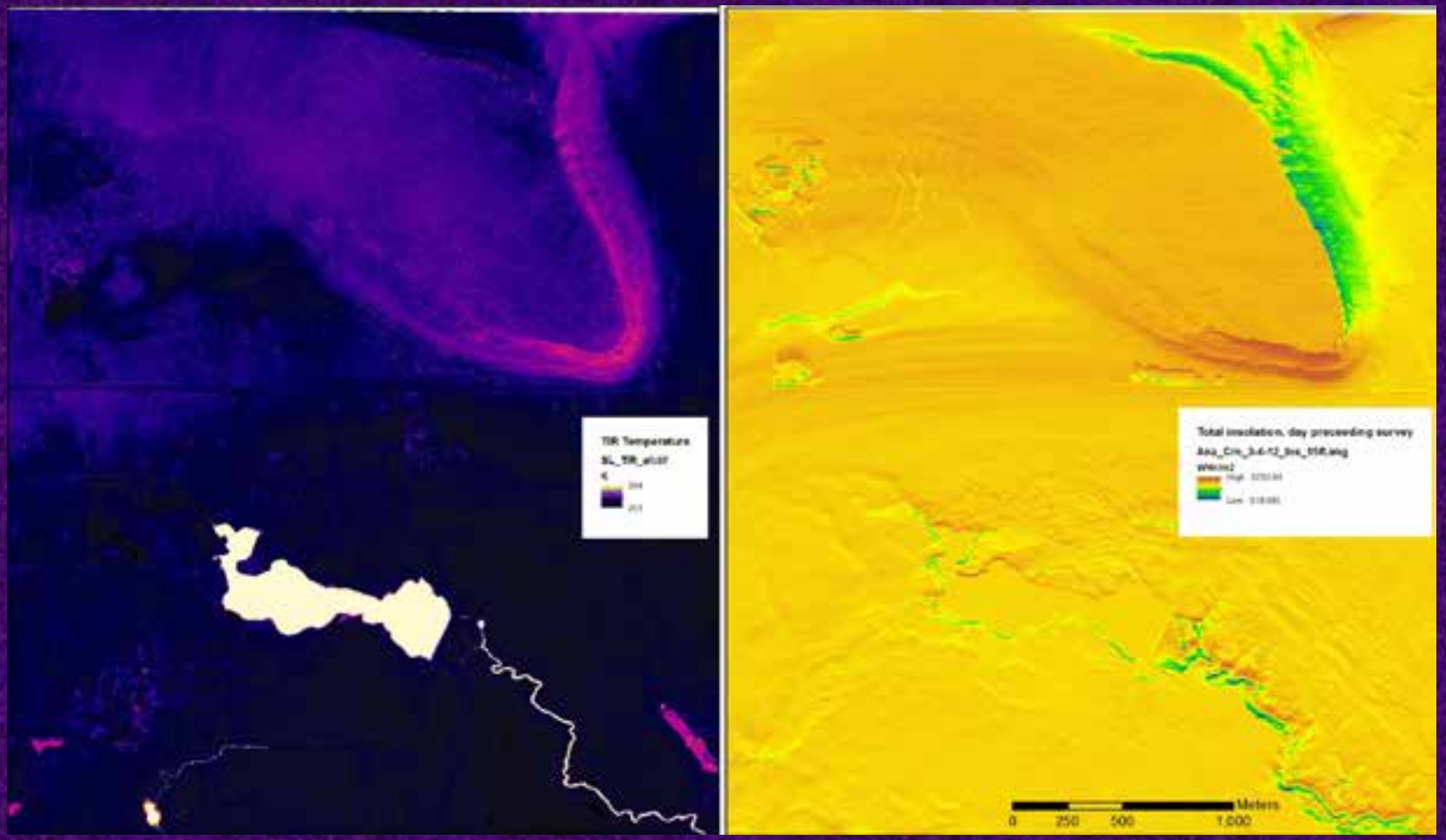

The registration between the lidar and TIR is excellent.

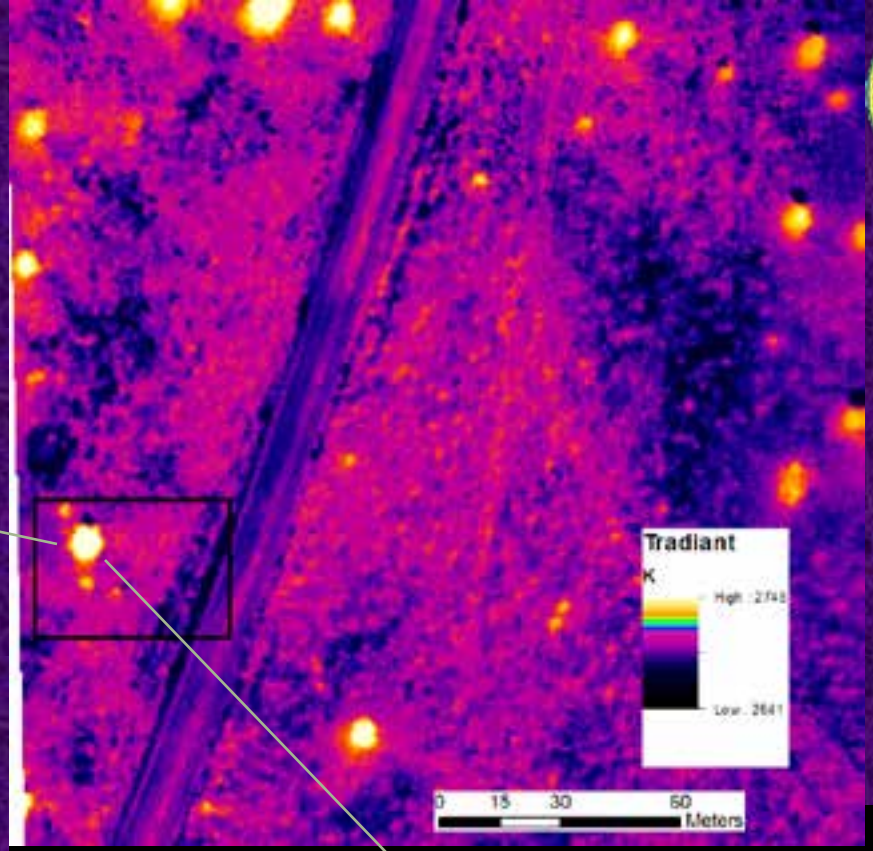

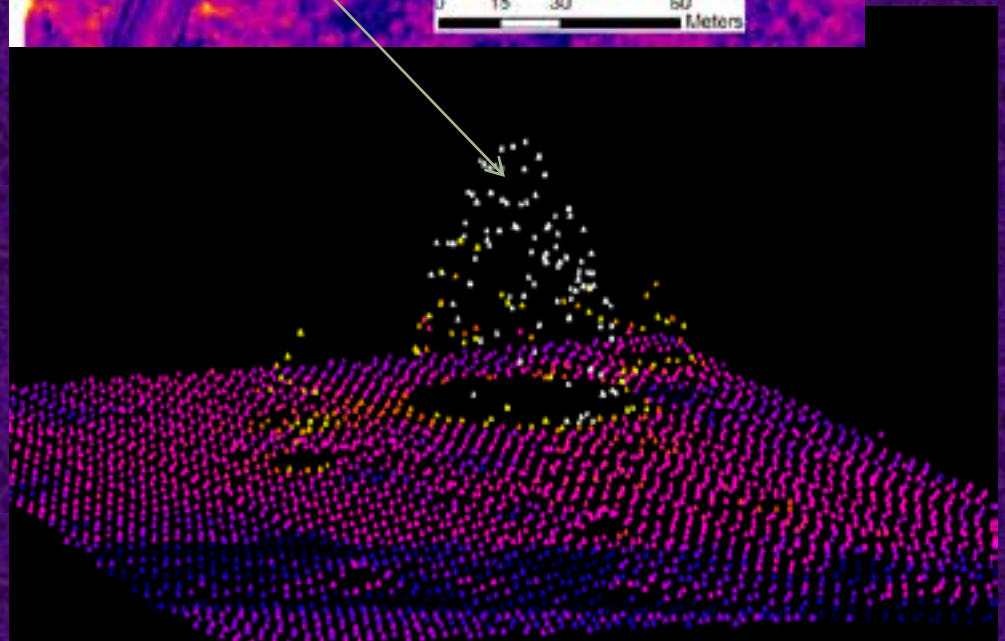

This means that we can identify features with different ε and either adjust the T_r map for ε, or more simply, mask out features we don't want to see.

ESRI UC 2014 Ian Madin

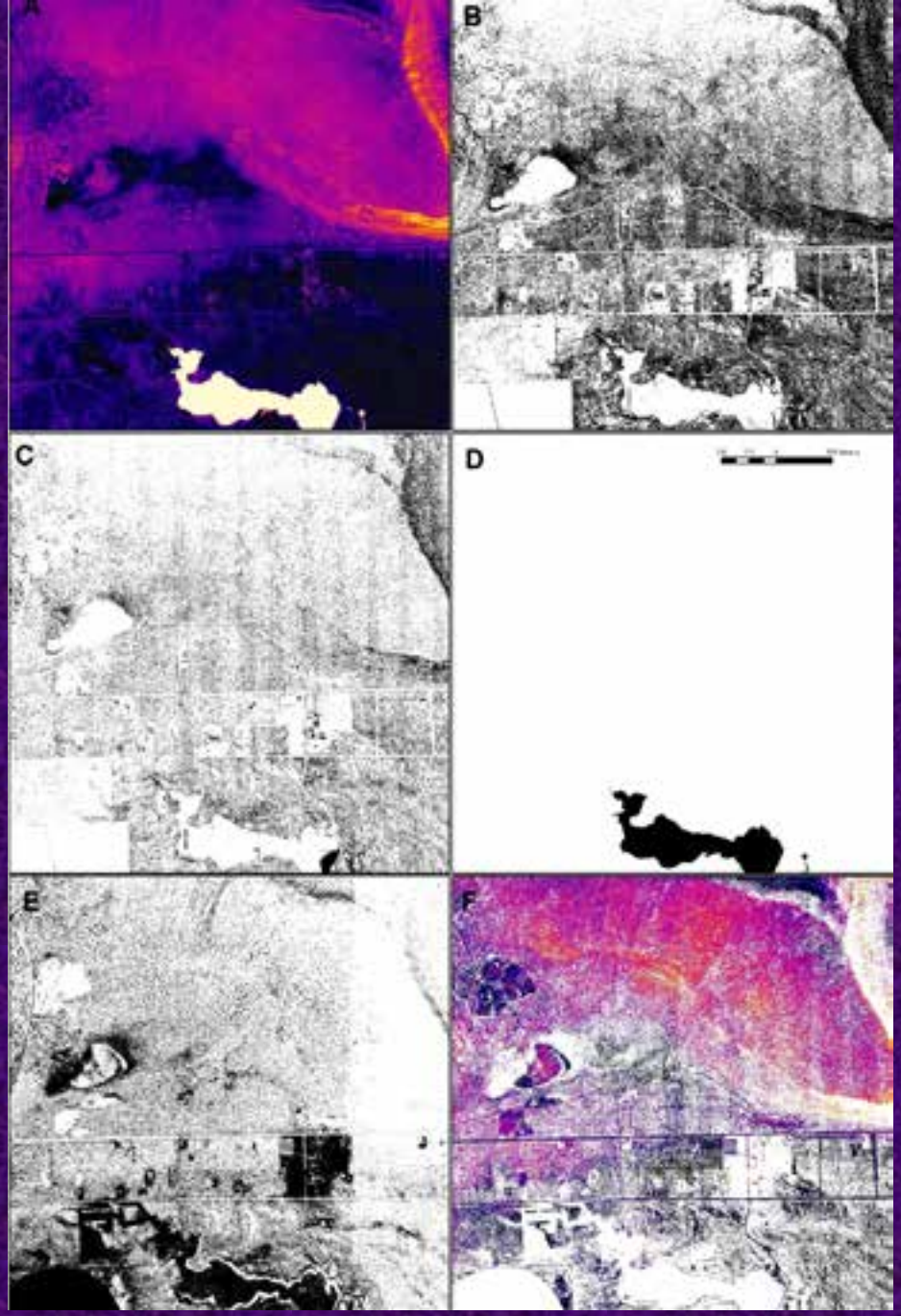

In order to remove the thermal signal of water and vegetation from the radiant temperature map (A) we used the lidar and orthoimagery to create vegetation and water masks. For vegetation we used canopy height (B) and surface roughness (C) and NDVI (E) and we digitized water bodies from orthoimagery (D). The masked radiant temperature image is shown in F.

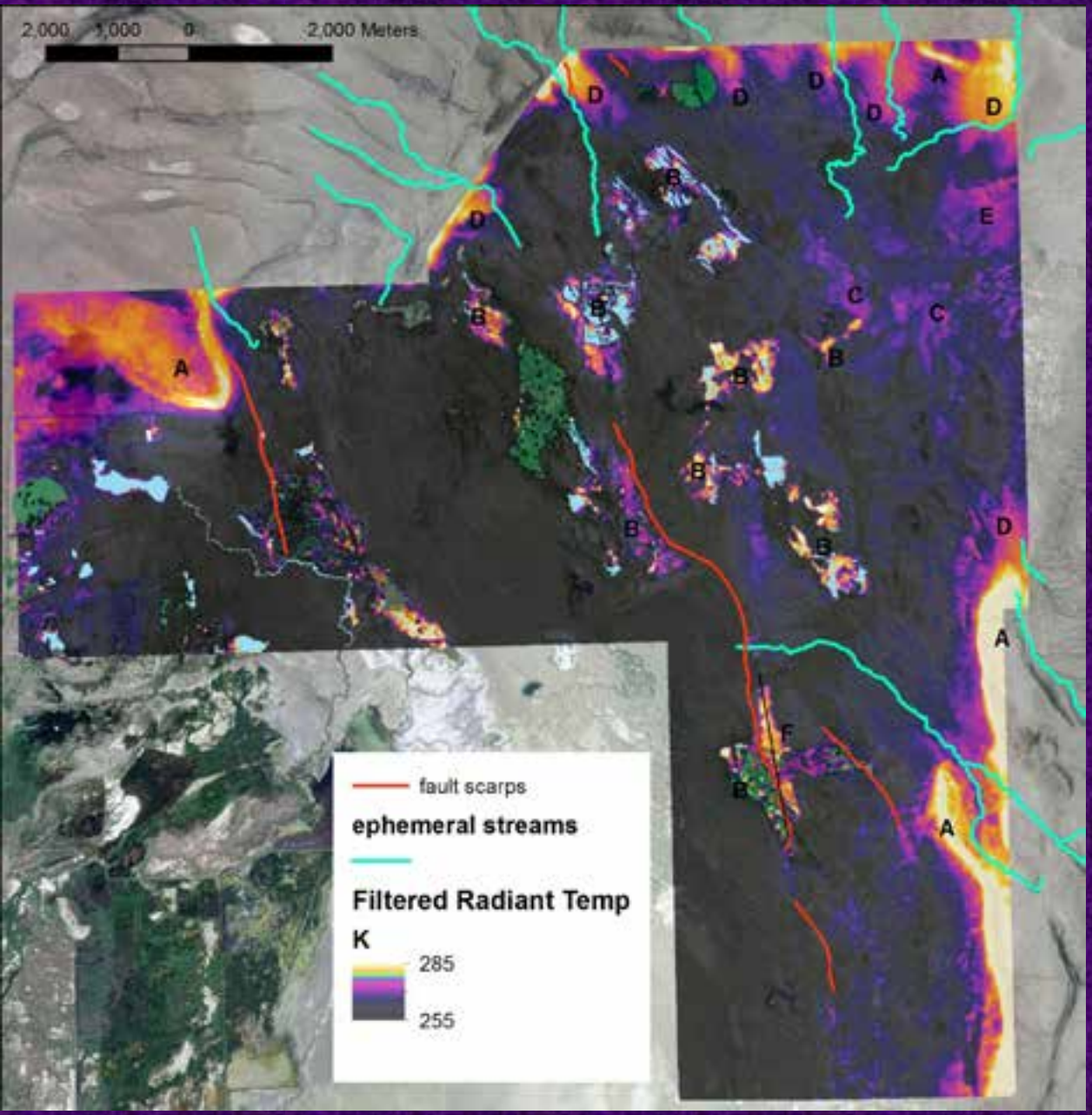

We used focal statistics to fill in the gaps in the masked radiant temperature image. We assumed that the geothermal anomalies would have long spatial wavelengths, so we used a 100m rectangular window. The filtered map allowed us to identify 6 classes of low thermal amplitude, long spatial wavelength anomalies.

Type A anomalies are 6-10 K above the surrounding areas and are associated with basalt bedrock at or near surface, and. Other areas are mantled with colluvium, beach gravel or lake sediment. The thermal conductivity of basalt is about three times higher than soil or gravel, so we speculate that these areas are warm because there is no insulating blanket of soil to trap deep heat flow.

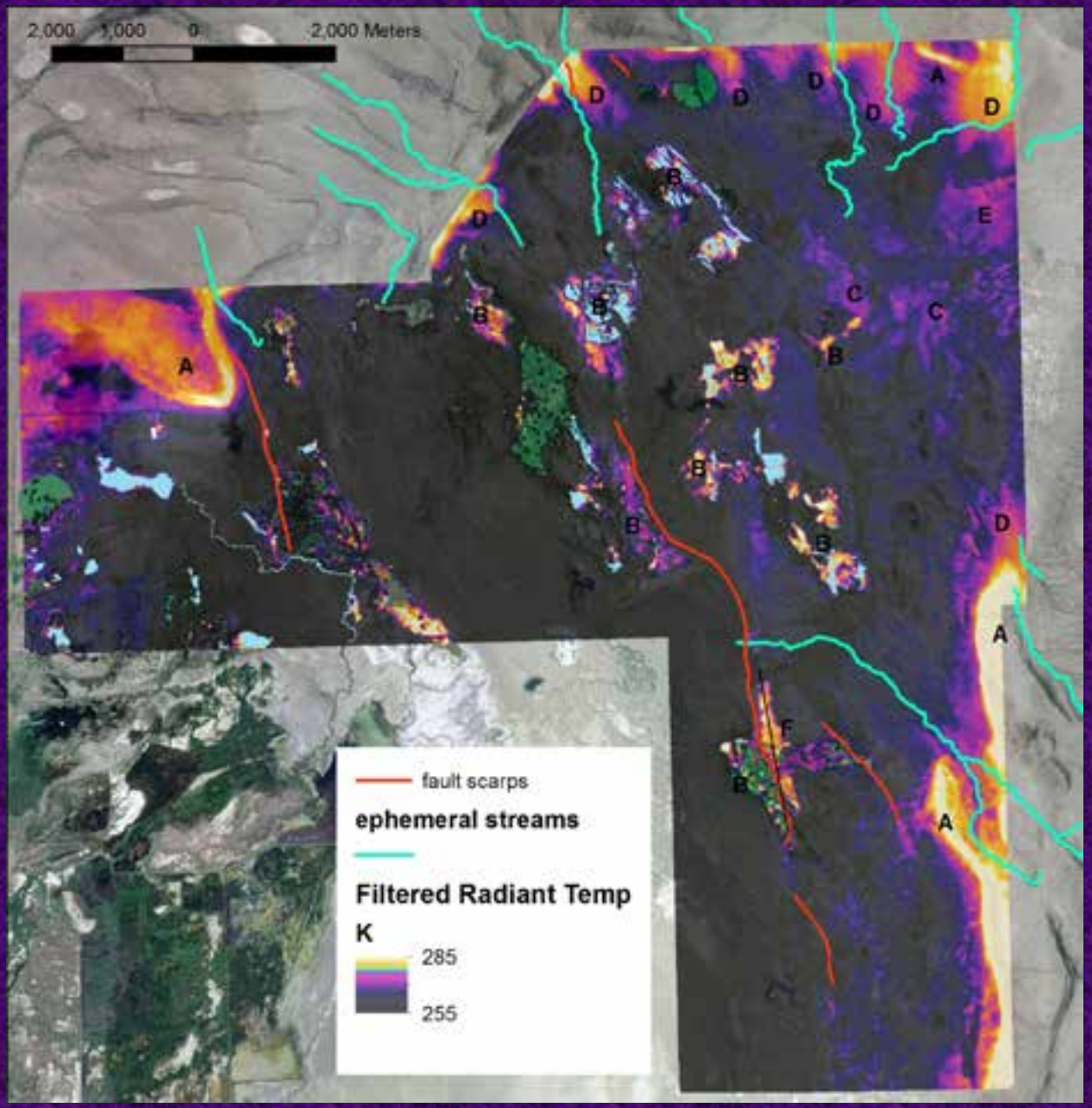

ESRI UC 2014 Ian Madin

Class B anomalies were associated with wetlands, and are due to incomplete masking. Liquid water has very low lidar intensity values, and also must be above 273k in temperature. The images below show the water mask (right light green) and a mask of low lidar intensity (left, light green) superimposed on areas of Tr > 273 (orange on both images). Using this combination of factors as a mask largely remove type B anomalies.

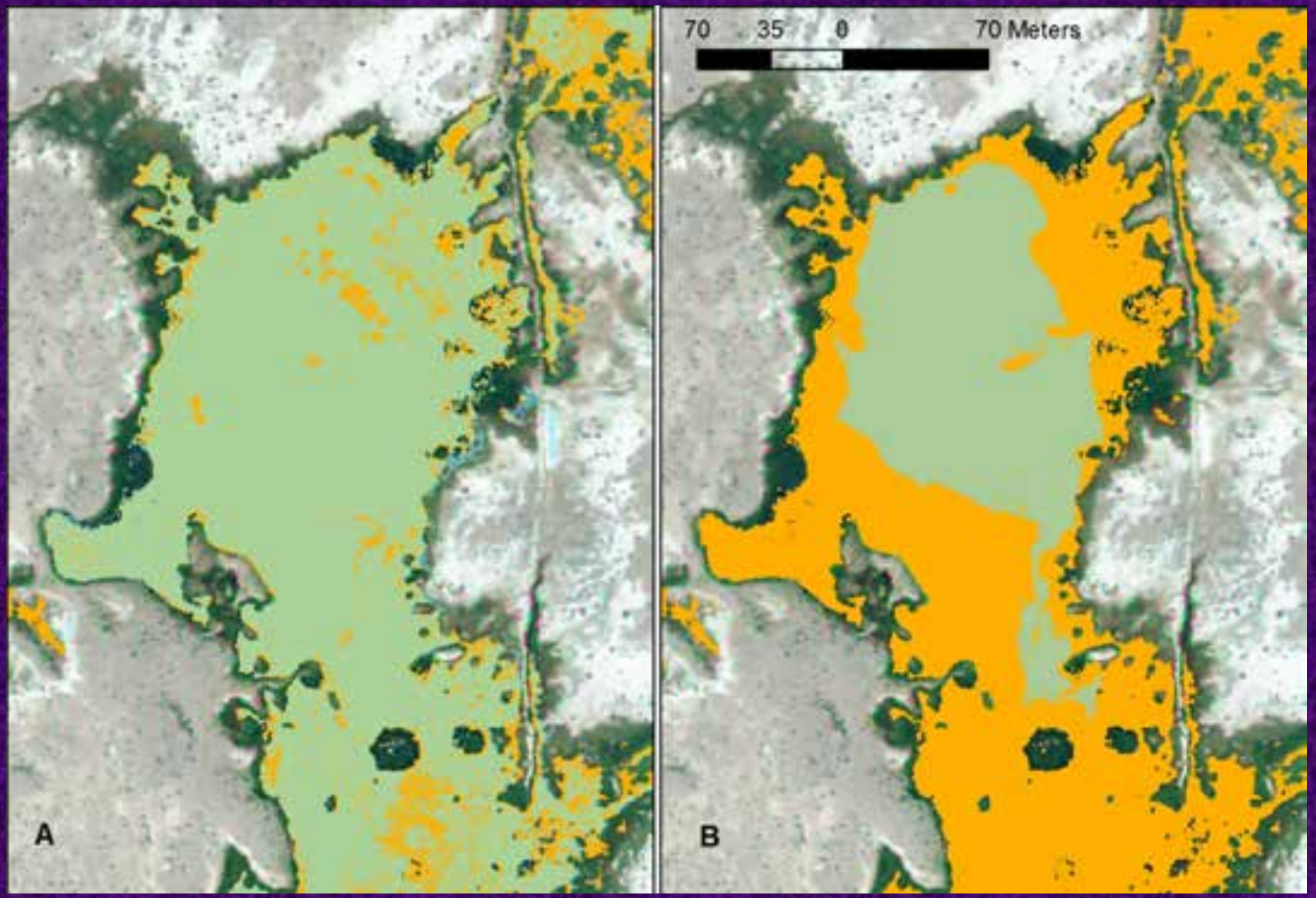

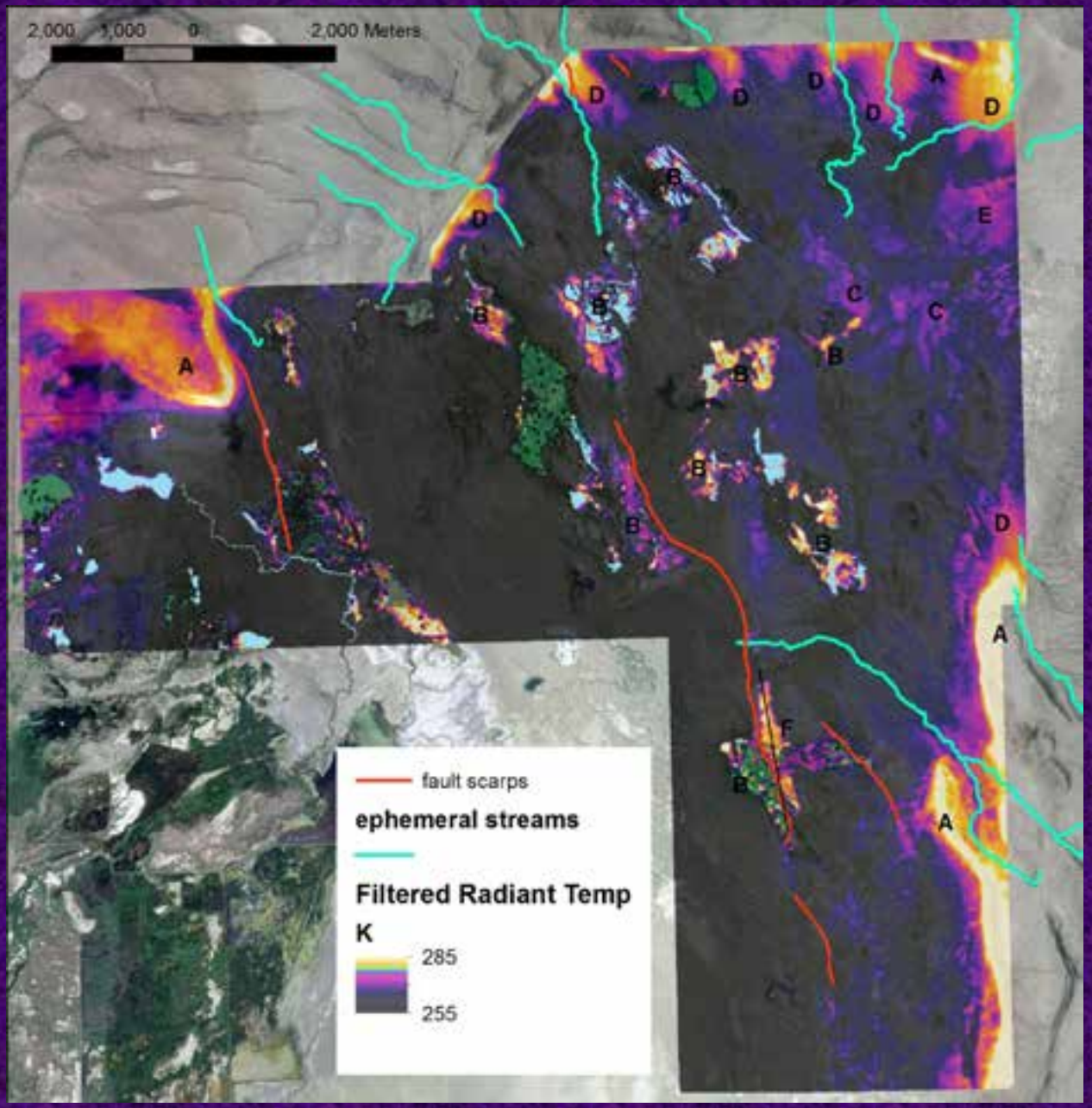

ESRI UC 2014 Ian Madin

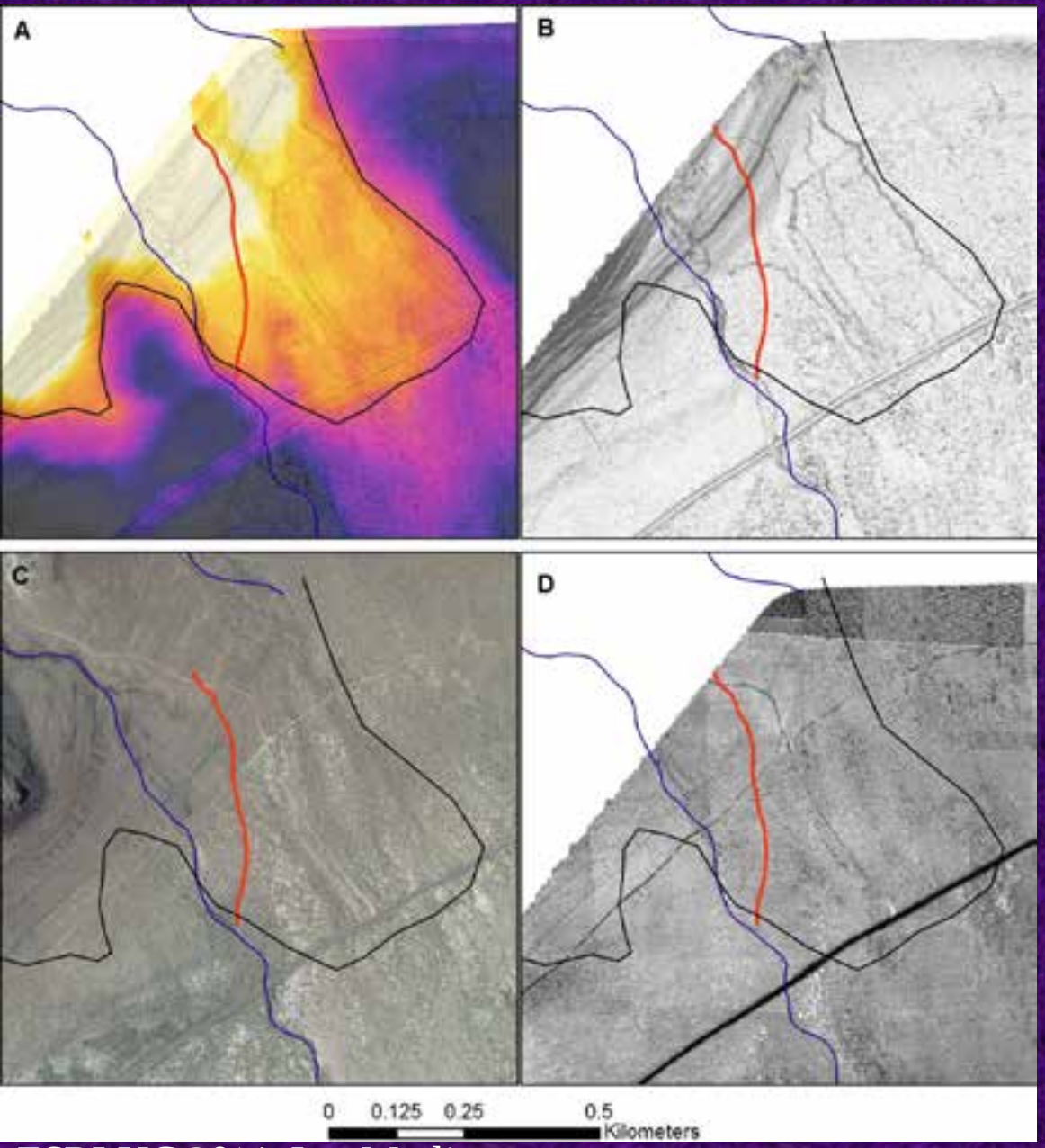

Type D anomalies (A) are typically about 5-8 K above the surrounding area. Their boundaries are not visible on lidar topography ((B), orthoimagery (C) and lidar intensity (D). We conclude that they truly represent warmer ground. They all occur where ephemeral stream channels enter the valley floor, and we speculate that the heat comes from shallow groundwater .

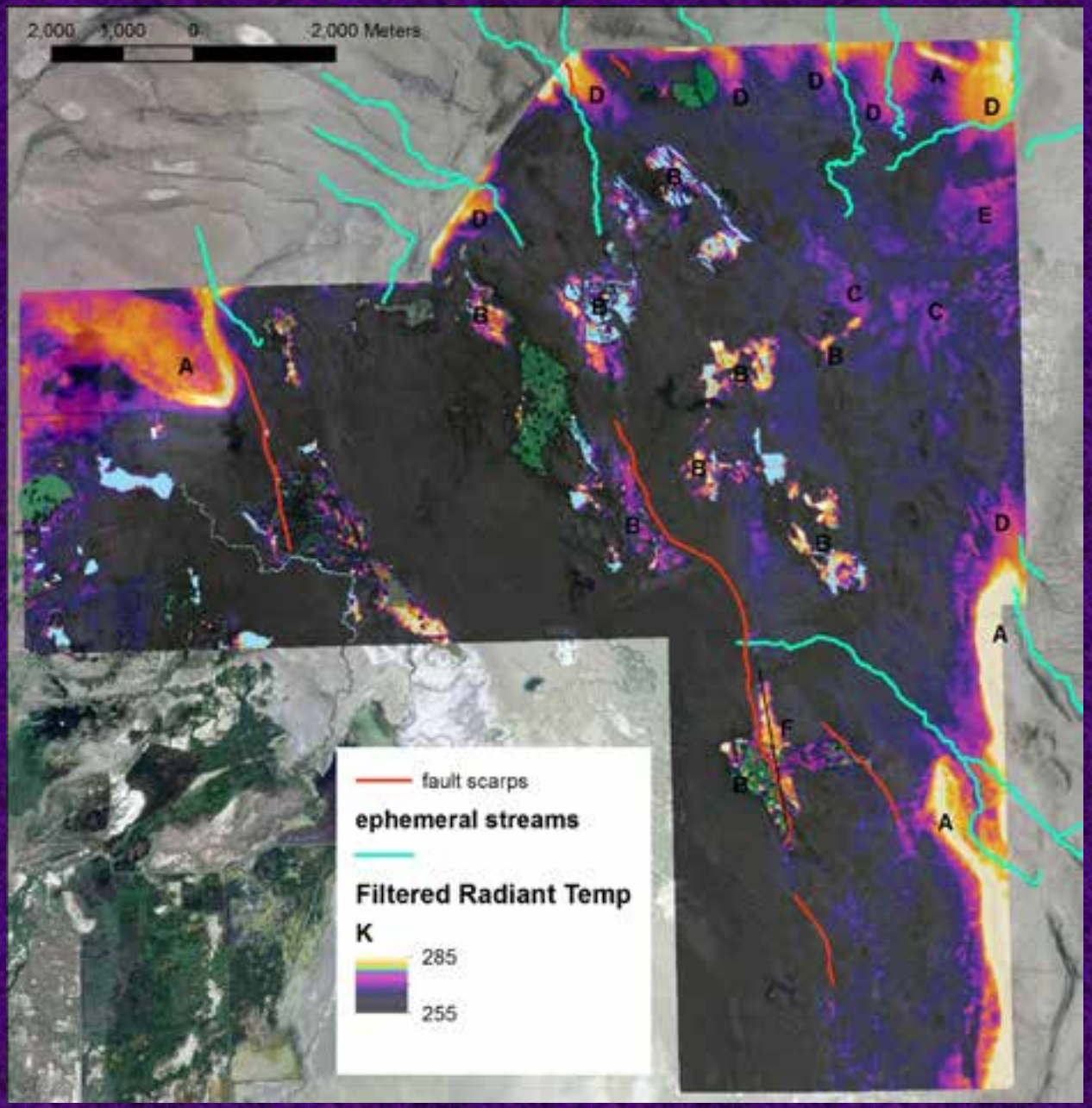

ESRI UC 2014 Ian Madin

The one Type F anomaly (A, Filtered T_r) was an area in the flat portion of the lake bottom that is 6-8 K above background. It is on the upthrown side of an active fault scarp discovered with the lidar, and adjacent to numerous warm springs (B). We believe this anomaly is due to geothermal water rising along the fault. This would be a good exploration target.

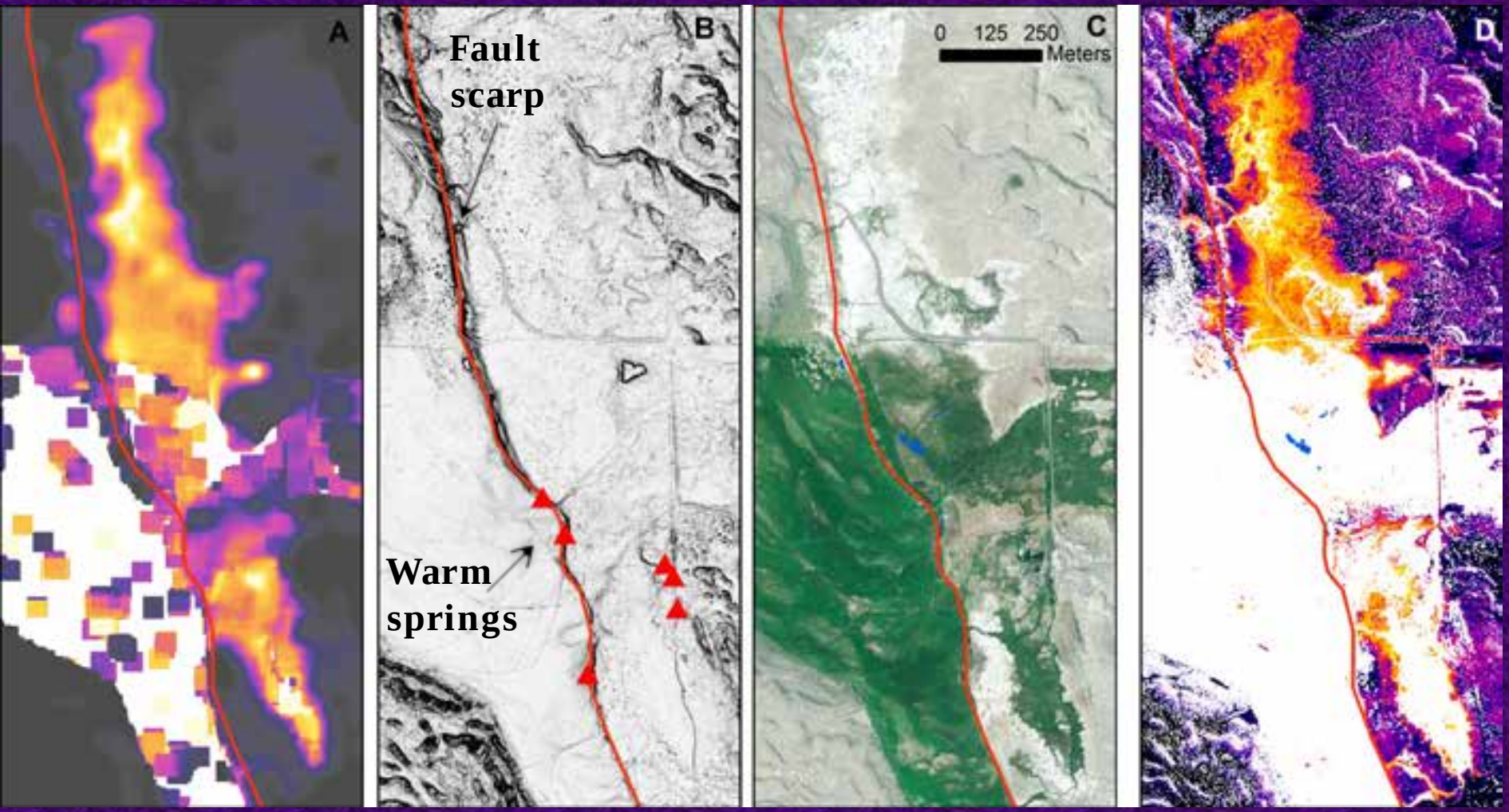

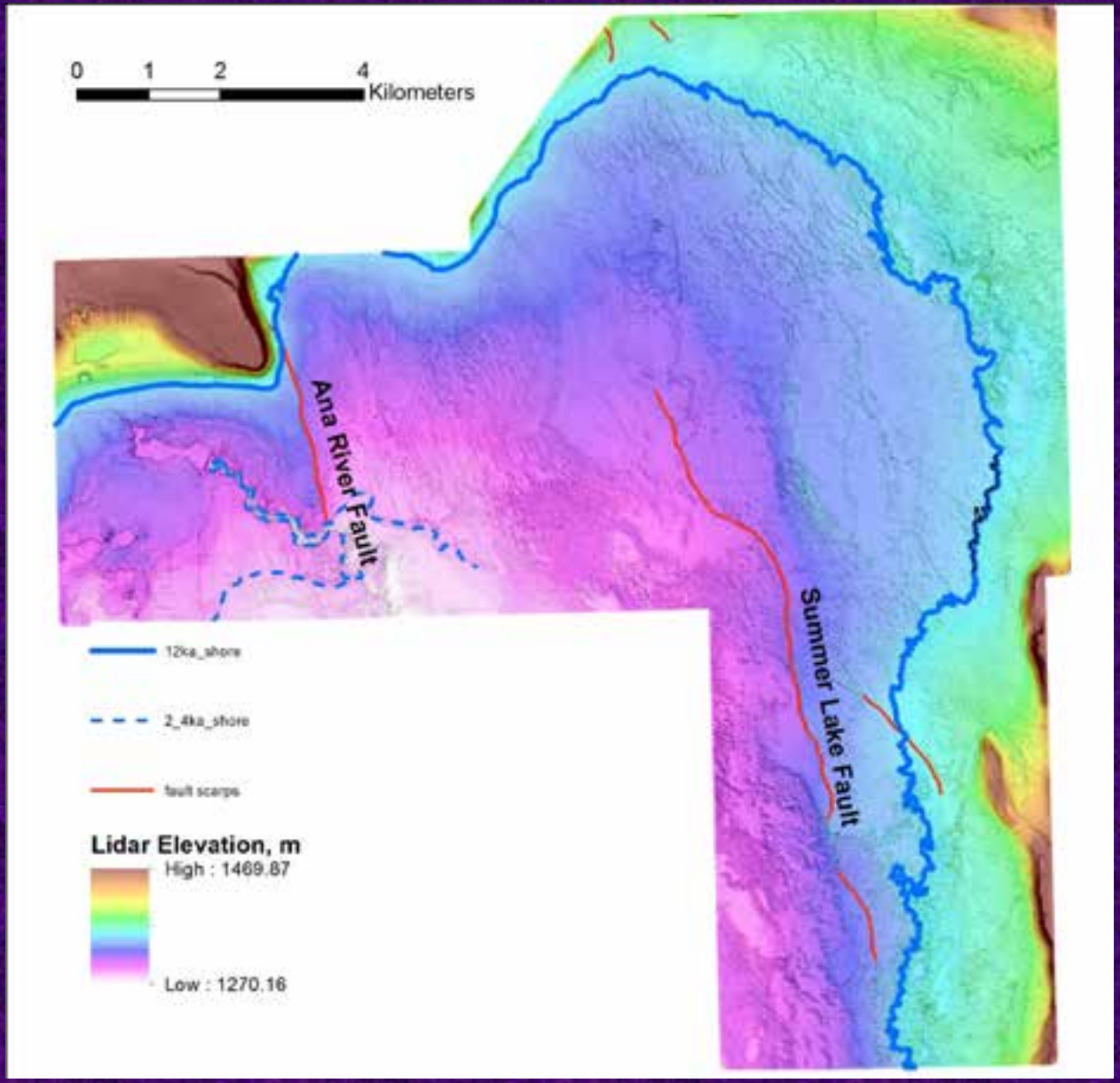

The lidar data revealed several previously unknown active fault strands. The lidar topography allowed us to show that the scarps were due to faults, not shorelines of the lake.

Summary

The addition of high resolution lidar to TIR data enhances the analysis of thermal sources, by making it possible to determine what features are producing the TIR signal.

The combined data set makes it possible to identify areas of anomalously warm ground.

The combined data set is an effective tool for locating and measuring warm and cold springs and for locating active faults.

Temperature depth profile of geothermal gradient hole drilled in NW corner of study area.